IDENTIFICATION AND VALIDATION OF DUCTILE DAMAGE PARAMETERS BY THE SMALL PUNCH TEST

Kuna, M., Abendroth, M.
Technische Universität Bergakademie Freiberg, Institute of Mechanics and Fluid Dynamics
Lampadiusstraße 4, 09596 Freiberg, Germany
e-mail: meinhard.kuna@imfd.tu-freiberg.de

Abstract

The small punch test (SPT) is a suitable miniaturized test method to determine the actual and local material state in structural components under operating conditions. A combined experimental-numerical approach is presented to identify material parameters of plastic deformation and ductile damage behaviour from the SPT. Neural networks (NN) are generated and trained by finite element simulations to obtain the relation between a load displacement curve of the SPT and the matching material parameters. These parameters, identified from SPT, are validated by reference values determined from smooth and notched tensile specimens. Next, the same parameters are used to simulate the ductile crack growth in fracture specimens by means of finite elements. This way, even fracture toughness data J_{Ic} of the materials could be successfully predicted. These findings substantiate the feasibility to gain comprehensive material characteristics from the SPT and their transferability to quantify the ductile failure of structural components.

Introduction

In recent years, different continuum damage models have been developed to describe ductile failure of metals, e. g. by GURSON-TVERGAARD-NEEDLEMAN (GTN) or ROUSSELIER, see the reviews [1, 2]. However, the determination of the material parameters involved in such models is still a challenging issue. Usually, smooth or notched tensile specimens are used to determine ductile damage parameters, whereby numerical simulations are suitably fitted to the experimental point of specimen failure, see e. g. [1, 2, 19]. More sophisticated techniques for parameter identification employ finite element analysis combined with gradient methods to minimise an error norm [18]. The application of neural networks to determine constitutive material properties was first demonstrated by [16].

On the other hand, ductile material behaviour in structural components is changing due to in service loading, irradiation, aging and other influences. That requires an in situ monitoring of the material state with ”minimal invasive” samples. Often local variations of material parameters have to be determined e. g. in weldments or gradient materials. Both motivations call for very small test specimens to be taken out of the material or component.

In the small punch test (SPT) a tiny disk-like specimen of ? 8? 0.5 mm size is deformed in a miniaturized deep drawing experiment, see Fig. 1 (left). The measurable output is the load displacement curve of the punch (Fig. 1, right), which contains information about the elastoplastic deformation and the damage behaviour of the material. The SPT was first introduced in the nuclear industries to monitor the degradation of material properties due to irradiation [3,4,5,6]. Mostly, empirical correlations were established between results from

small punch tests (yield stress, ultimate strength, fracture energy) and conventional specimen data to find out the shift of the ductile to brittle transition temperature. The SPT was also used to determine the elastic plastic hardening properties [7, 8]. Some researchers attempted to obtain the brittle K_{Ic} or ductile fracture toughness J_{Ic} [9, 10]. Recently, the potential of ductile damage mechanics was applied to investigate and interpret SPT with respect to ductile deformation and failure behaviour [11-13].

Experiments

In the SPT testing device, the specimen is clamped between die and down-holder. A punch with spherical head is centrically moved downwards with prescribed low velocity. Thereby the vertical displacement u (= deformation of the specimen) of the punch and the acting force F are measured. More detailed information about the experimental setup can be found in [11]. The dimensions are h =0.5mm, D = 8mm, d = 4mm, r = 0.5mm, R = 1.25mm. A typical load displacement curve (LDC) is shown in Fig. 1, which can be split up into several parts. Part I is mainly determined by the elastic properties of the material, Part II reflects the transition between the elastic and plastic behaviour, Part III shows the hardening properties up to part IV, where geometrical softening and damage occurs. During the steep decent in Part V the specimen fails by ductile crack growth along a concentric ring. The SPT-specimens have to be carefully manufactured from rods by slicing on a diamond saw and stepwise grinding and polishing to the exact thickness [11]. Two different reactor pressure vessel steels are investigated, the Russian type 18Ch2MFA (WWER 440) and the German one 22NiMoCr37.

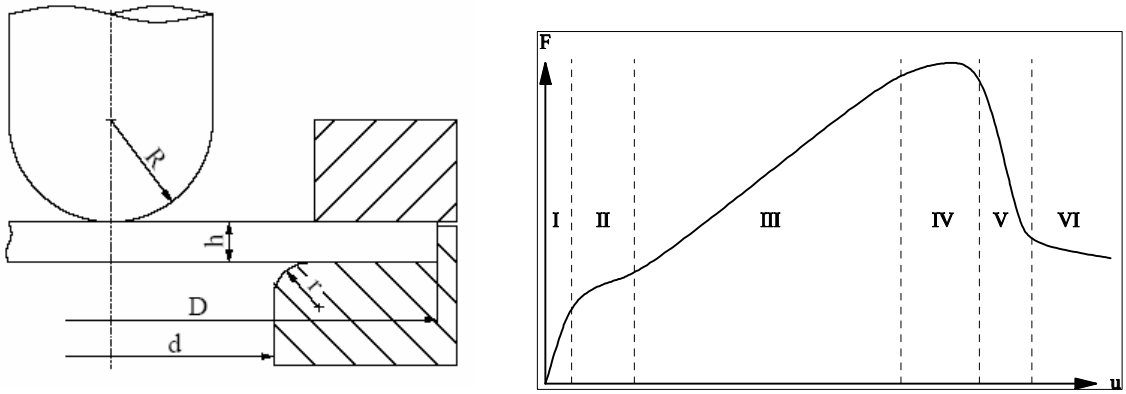

FIGURE 1. Schematic drawing of the Small Punch Test and the load displacement curve

In order to verify the material parameters obtained by the SPT, tensile tests with round notched specimens are carried out additionally for the material 18Ch2MFA (D = 12mm, d_0 = 6mm, L = 80mm, $l_0 \approx$ 20mm). To adjust different values of stress triaxiality, the notch radii are varied r =1, 2, 4, 8mm, see [12]. Reference data for the steel 22NiMoCr37 are taken from the report [19].

Numerical Analysis

The constitutive damage law developed by GURSON-TVERGAARD-NEEDLEMAN (GTN) is used to describe an elastic plastic continuum with spherical voids [1], which can nucleate, grow and coalesce. The damage is quantified by the void volume fraction f. This well known model is briefly outlined in order to introduce the relevant material parameters. The yield

function is formulated in equivalent $\Sigma_V = \sqrt{\frac{3}{2}\Sigma'_{ij}\Sigma'_{ij}}$ and mean hydrostatic $\Sigma_H = \frac{1}{3}\Sigma_{kk}$ stresses

$$\Phi = \left(\frac{\Sigma_V}{s_F(e_{pl})} \right)^2 + 2q_1 f^* \cosh\left(\frac{3}{2} q_2 \frac{\Sigma_H}{s_F(e_{pl})} \right) - \left(1 + q_3 f^{*2}\right) = 0 \ . \qquad (1)$$

The isotropic hardening of the matrix material $s_F(e_{pl})$ is represented by the following power law for the actual true yield stress s_F versus equivalent plastic strain e_{pl}

$$s_F(e_{pl}) = R_e \left[\frac{e_{pl}}{e^*} + 1 \right]^{\frac{1}{n}} \quad \text{with} \quad e^* = \left[\left(\frac{s^*}{R_e} \right)^n - 1 \right]^{-1} \quad \text{and} \quad s^* = s_F(1). \qquad (2)$$

Here, the parameters are initial yield stress R_e , hardening coefficient n and s^*. Above a critical porosity f_c an accelerated void growth occurs, which is described by the modified damage variable f^* related to the true void volume fraction f by the bi-linear form

$$f^* = \begin{cases} f & f \le f_c \\ f_c + k(f - f_c) & f > f_c \end{cases} \quad \text{with} \quad k = \frac{f_u^* - f_c}{f_f - f_c} \quad \text{and} \quad f_u^* = \frac{1}{q_1} \ . \qquad (3)$$

f_f represents the critical void volume fraction at macroscopic failure. Furthermore, a nucleation term is introduced with quantities f_N, e_N and s_N.

$$\dot{f}_{nucl} = A\dot{e}_{pl} \quad \text{with} \quad A = \frac{f_N}{s_N\sqrt{2p}} \exp\left[-\frac{1}{2}\left(\frac{e_{pl} - e_N}{s_N} \right)^2 \right]. \qquad (4)$$

Together with the initial void volume fraction f_0 and the adjusting parameters q_1, q_2 and q_3, the complete constitutive model comprises 12 parameters

$$\{par_i\} = \{R_e, n, s^*, q_1, q_2, q_3, f_0, f_c, f_N, f_f, e_N, s_N\}. \qquad (5)$$

The implementation of the GTN-model [15] in the finite element code ABAQUS was used to analyse all investigated test specimen types. According to previous investigations [11], the optimal finite element model for the SPT is shown in Fig. 2. Since geometry and loading of the SPT are axisymmetric, a two dimensional model with axisymmetric reduced integration elements is sufficient. The die, down-holder and punch are modelled as rigid bodies, taking frictional contact to the specimen into account with a friction coefficient m = 0.12. The punch was moved vertically by a displacement boundary condition. Since numerical damage analyses are known to be sensitive to discretisation, for all computed specimen types one and the same element size of 0.1? 0.1mm was employed throughout. In Fig. 2 (left) the distribution of void volume fraction f is depicted on the deformed SPT, whereas one notched tensile specimen at intermediate load level is shown right.

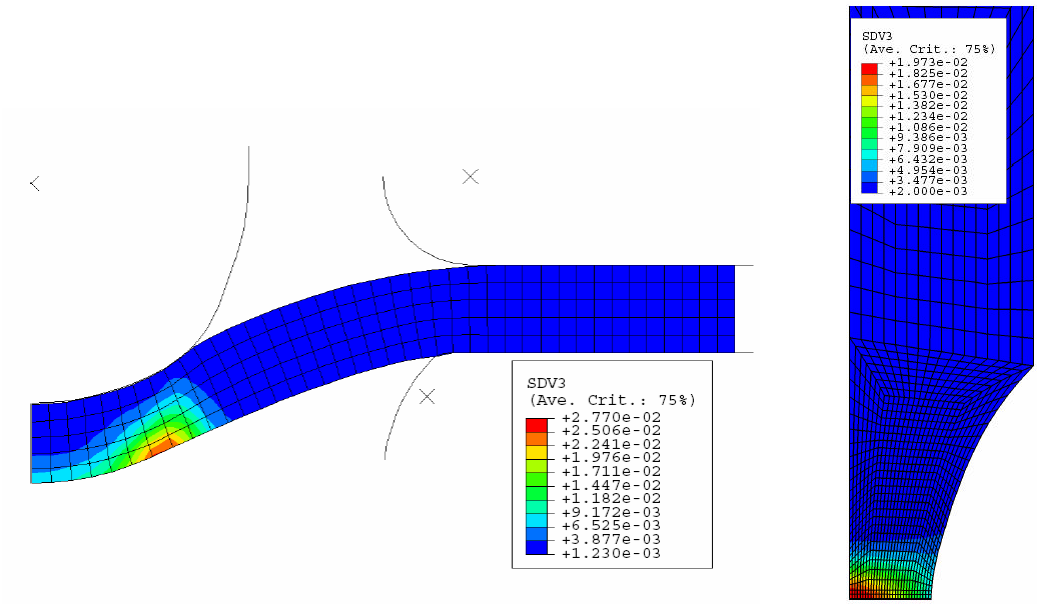

FIGURE 2. Finite element models with damage distributions of the Small Punch Test (left) and of a notched tensile specimen (right) for 18Ch2MFA

Parameter Identification by Neural Networks

To identify the hardening and damage parameters listed in Eq.(5), a unique correlation between the LDC *F(u)* of the SPT and the corresponding material parameters par_i has to be established. The LDC can be regarded as a function (6) for the punch force F depending on the displacement u and the material parameters par_i. This function is created by systematic forward FEM-calculations with varying parameter sets and stored in a knowledge base. For parameter determination, the inversion of this mapping is searched, which could be successfully performed by means of Neural networks (NN) in [11, 12]. The used NNs belong to the class of multi-layer perceptrons (see [14]), which consist of three layers of neurons, forming input, hidden and output level.

$$F(u) = f(par_i) \qquad \leftrightarrow \qquad par_i = j(F(u)) \tag{6}$$

Now, special NNs can be generated and trained by the FEM data base. During the training process, data pattern are feed into the NN and its output values are compared with the known true data. These special learning algorithms [14, 12] are repeated, until an error norm is minimised. By independent validation patterns the quality of the NN is then approved.

Two different approaches were elaborated to find par_i.

Approach I: Create the inverse function j by a NN (direct identification). The simulated LDCs serve as input of the NN and the material parameters are replied as output, see [11, 12]. In general this technique works well, but it becomes unfavourable if redundancy among the material parameters appear leading to non-uniqueness of results.

Approach II: Here, a NN is generated to give an approximate solution for the direct function f of Eq. (6). This means, if a given punch displacement u and parameter set par_i are put into the NN, the force response $F'(u) = f'(par_i)$ of the SPT is put out. The great advantage is that the NN can be used now instead of extensive FEM-calculations. To find the true parameter set for an experimental LDC *F(u),* it is compared with the answer *F'(u)* from the NN for an initially given set par_i'. By a nonlinear optimisation procedure the parameters are

improved until the error $err = \left\| F(u) - F'(u)\,|_{par_i} \right\| \rightarrow Min$ falls below a margin. The optimisation algorithm with conjugate directions of [17] is used for this minimisation.

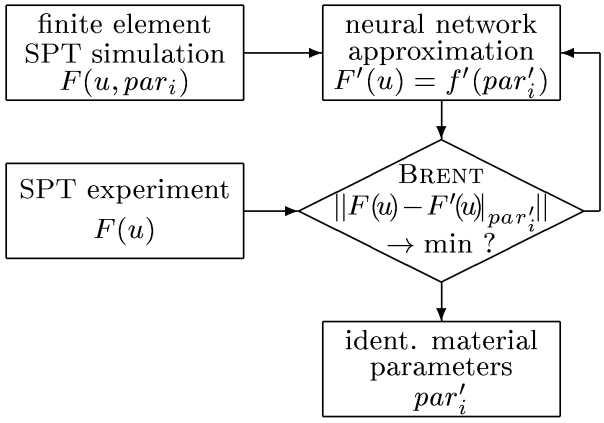

FIGURE 4. Scheme of the identification approach II

TABLE 1. Fixed and identified material parameters for SPT

	18 Ch2MFA (M=5)			**22 NiMoCr37** (M=6)		
Parameter		**Variation**	**Value**		**Variation**	**Value**
Re	identified	200-700	**650.7**	fixed	430	**430**
n	identified	5-15	**5.85**	fixed	6.44	**6.44**
s *	identified	800-1300	**1032**	identified	900-1000	**982**
f_0	fixed	0.002	**0.002**	fixed	0.002	**0.002**
f_c	identified	0.05-0.18	**0.122**	identified	0.05-0.15	**0.102**
f_f	fixed	0.2	**0.2**	fixed	0.2	**0.2**
f_N	identified	0.01-0.03	**0.0138**	identified	0.01-0.05	**0.05**
e_N	fixed	0.3	**0.3**	fixed	0.3	**0.3**
s_N	fixed	0.1	**0.1**	fixed	0.1	**0.1**
q_1	fixed	1.5	**1.5**	identified	0.80-1.20	**0.846**
q_2	identified	1.00-1.20	**1.114**	identified	0.70-1.20	**1.03**
q_3	fixed	2.25	**2.25**	fixed	q_1^2	$\boldsymbol{q_1^2}$

Results for the Small Punch Test

The explained approach II was applied to the SPT of both steels. To reduce the effort of parameter identification, not the total number of all 12 free parameters was considered. Instead, from certain reasons specific parameters are fixed to known or reasonable values.

For instance, for 18Ch2MFA the initial porosity f_0 could be estimated from chemical content of manganese and sulphur [2]. For 22 NiMoCr37 the hardening data and f_0 were specified in [19]. The influence of e_N and s_N is usually of less importance, so standard values from literature were taken. Thus, only M parameters are chosen to be adjusted, whereas the other are kept fixed. The fixed and variable parameters, their values and assumed intervals are listed in Table 1 for both steels. The complete identified parameter sets (printed in bold letters) prove good agreement with the original SPT experiments, as can be seen from Fig. 5. The necessary data bases created by FEM amounted to about M^5 calculations. The corresponding NNs had $(M+1)$ input neurons and 1 output neuron (force).

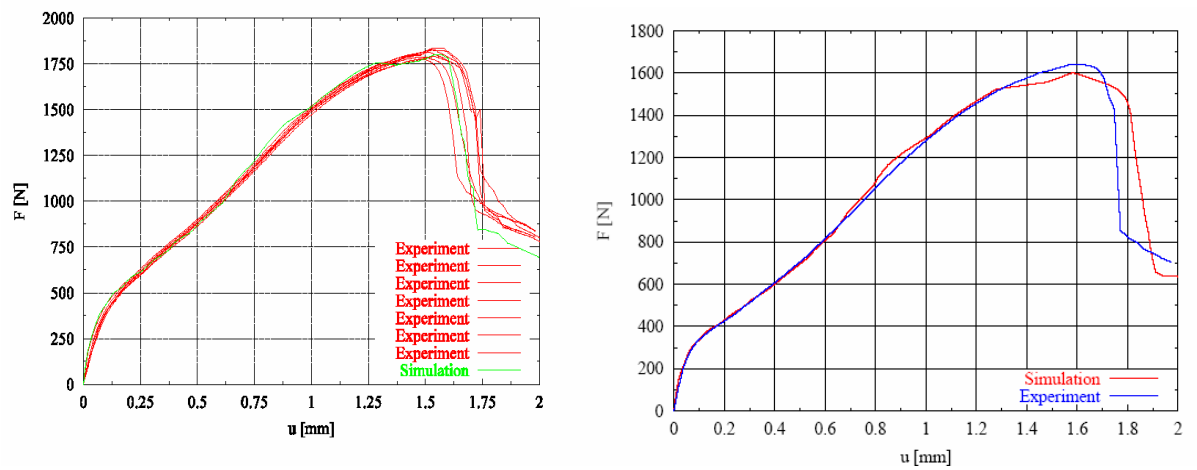

FIGURE 5. Comparison of measured and simulated LDCs for the SPT with identified material parameters: 18Ch2MFA (left), 22NiMoCr37 (right)

Validation by Notched Tensile Tests

Using the parameters obtained from SPT, notched tensile tests have been simulated for both materials. The simulations predicted the behaviour of the experiments reasonably well, see Fig. 6. This holds even for varying triaxialities, encountered for different notch radii with 18Ch2MFA. Fig. 6 (right) compares the simulation with two experiments given in [19].

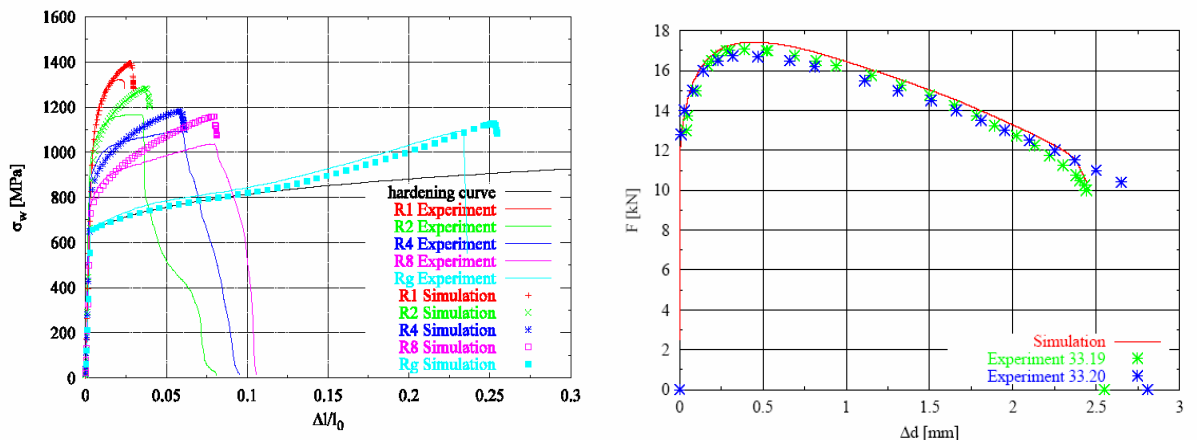

FIGURE 6. True stress versus elongation for different notched tensile tests of 18Ch2MFA (left) and force-necking-curve for smooth tensile test of 22NiMoCr37 (right)

Transfer to Fracture Test Specimens

As a next step, the transferability of SPT material parameters to fracture mechanics test specimens ought to be validated. In Müller [20] the steel 18Ch2MFA was characterised by fracture tests of single edge notched specimen (SENB) of the dimensions B = 10 mm, L = 80mm and initial crack length a_0 = 10mm. Therefore, the SENB-specimens under four-point bending was analysed. Because of 20% side grooves a plane strain state could be expected, allowing a two-dimensional FEM analysis. Fig. 7 depicts one half of the finite element discretisation and the distribution of v. Mises equivalent stress. The stable ductile crack growth is simulated automatically by the damage model and leads to a chain of failed elements along the ligament. The detail in Fig. 7 shows the advancing crack. The far field J-integral was computes simultaneously for all load steps, thus the crack growth resistance curve J-Da can be recorded. The experimental J-Δa curve is compared with the simulated one in Fig. 8. The agreement is quite sufficient, which allows the conclusion that the parameter set gained from SPT is generally valid for this steel.

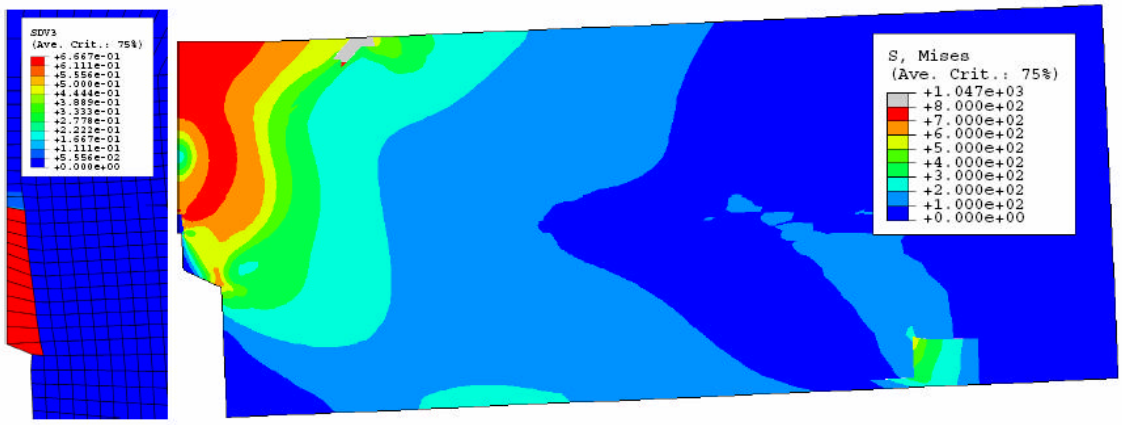

FIGURE 7. Damage zone due to crack growth (left) and equivalent stress (right) 18Ch2MFA

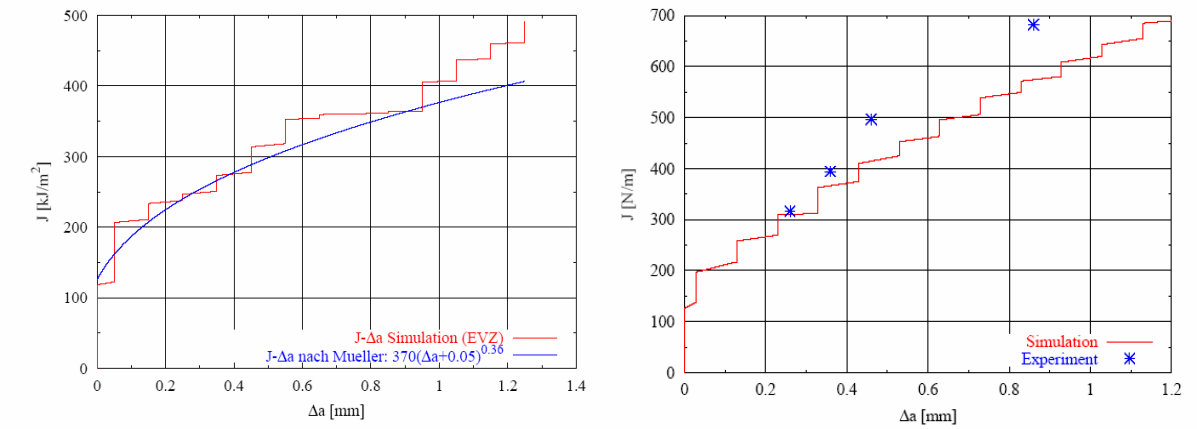

FIGURE 8. Experimental and simulated crack resistance curves for steels 18Ch2MFA (left) and 22NiMoCr37 (right)

This statement was also confirmed by a similar analysis, carried out for fracture tests of 22NiMoCr37 with CT-specimens. Specimen geometry and test results are reported in [19]. As can be seen in Fig. 8 (right), the measured J-Δa curve is very well predicted by the simulations. Especially the important initiation values J_{Ic} match the experiments excellently.

Conclusion

It could be proved that the SPT is a suitable testing method to determine hardening and damage parameters of ductile materials. Due to its extremely small sample volume, the SPT is qualified to examine local and current material properties. The validity and transferability of SPT-results was checked by data of large specimens commonly used for materials testing in damage mechanics. Furthermore, by numerical simulation of ductile crack growth in fracture specimens, even fracture toughness values could be successfully deduced.

References

1. Tvergaard, V., in Mechanical Behaviour of Materials, edited by A. Bakker, Delft University Press, 1995, 23-43.
2. Kussmaul, K. et al., *Proc. Int. Seminar on Local Approach of Fracture, Nuclear Engineering & Design*, vol. **105**, 1-156, 1987.
3. Manahan, M., Argon, A., Harling, O., *Journal of Nuclear Materials,* vol. **103-104,** 1545-1550, 1981.
4. Baik, J.-M., Kameda, J. and Buck, O., *Scripta Metallurgica*, vol. **17**, 1443-447, 1983.
5. Foulds, J. et al., Steam Turbine-Generator Developments for the Power Generation Industry American Society of Mechanical Engineers, Power Division (Publication) PWR, Publ. by ASME 18 (1992) 151-157.
6. Jitsukawa, S. et al., *ASTM Special Technical Publication*. vol. **1204**, 289-07, 1993.
7. Fleury, E., Ha, J., *Int. Journal of Pressure Vessels and Piping*, vol. **75**, 699-706, 1998.
8. Sainte Catherine, C. et al., *Small Specimens Test Techniques*, vol. **4**, 350-370, 2002.
9. Bulloch, J., *Int. Journal of Pressure Vessels and Piping*, vol. **75**, 791-804, 1998.
10. Mao, X., Saito, M. and Takahashi, H., *Scr Metall Mater*, vol. **25**, 2481-2485, 2000.
11. Abendroth, M., Kuna, M., *Computational Materials Science*, vol. **28**, 633-644, 2003.
12. Abendroth, M., Kuna, M., in: *DVM-Bericht 235, Fortschritte der Bruch- und Schädigungsmechanik*, 2003, 269-278.
13. Abendroth, M., Kuna, M., Determination of Ductile Material Properties by Means of the Small Punch Test and Neural Networks, *Advanced Engineering Materials* 2004, accepted for publication.
14. Zell, A. et al., SNNS Stuttgart Neural Network Simulator, User Manual V. 4.1, 1995.
15. Mühlich, U., Brocks, W. and Siegmund, T., Technical note gkss/wmg/98/1, GKSS-Forschungszentrum Geesthacht (1998).
16. Huber, N., Tsakmakis, Ch., *J. Mech. Phys. Solids*, vol. **47**, 1589-1607, 1999
17. Brent, R. P., Algorithms for Minimization Without Derivatives, Prentice-Hall, Englewood Cliffs, N.J., 1973.
18. Mahnken, R., *International Journal of Plasticity*, vol. **15**, 1111–1137, 1999.
19. Bernauer, G., Brocks, W., *Numerical round robin on micromechanical models, Phase II, Task B1*, Technical report, ESIS European Structural Integrity Society, 1999.
20. Müller, K., PhD thesis, TU-Bergakademie Freiberg, 1994.